Published in final edited form as:
Neuroscience. 2008 August 26; 155(3): 948–958. doi:10.1016/j.neuroscience.2008.06.024.

Inflammatory Pain-Induced Signaling Events Following a Conditional Deletion of the N-Methyl-D-Aspartate Receptor in Spinal Cord Dorsal Horn

Hsinlin T Cheng, **Masahiro Suzuki**, **Deborah M Hegarty**, **Qinghao Xu**, **Amanda R Weyerbacher**, **Samantha M South**, **Megumi Ohata**, and **Charles E Inturrisi**
Departments of Pharmacology (H.T.C., M.S., S.M.S., M.O., C.E.I.) and Neuroscience (D.M.H., Q.X., A.R.W), Weill Medical College, Cornell University, and Department of Neurology, Memorial Sloan Kettering Cancer Center, New York, New York 10021 (H.T.C., C.E.I.)

Abstract

The N-methyl-D-aspartate (NMDA) receptor in the spinal cord dorsal horn (SCDH) is one of the mechanisms involved in central sensitization during chronic pain. Previously, this laboratory created a spatio-temporal knockout (KO) of the NMDA receptor I (NR1) subunit in the mouse SCDH. The NR1 KO completely blocks NR1 gene and subsequent NMDA receptor expression and function in SCDH neurons. In the NR1 KO mice, the mechanical and cold allodynia induced at 24 h after Complete Freund's adjuvant (CFA) was reduced. However, the protective effects of KO were transient and were not seen at 48 h after CFA. These observations suggest the presence of NMDA-independent pathways that contribute to CFA-induced pain. CFA induces the activation of several signaling cascades in the SCDH, including protein kinase C (PKC)γ and extracellular signal-regulated kinases (ERK1/2). The phosphorylation of PKCγ and ERK1/2 was inhibited in the SCDH of NR1 KO mice up to 48 h after CFA treatment, suggesting that these pathways are NMDA receptor-dependent. Interestingly, neuronal cyclooxygenase (COX)-2 expression and microglial p38 phosphorylation were induced in the SCDH of the NR1 KO at 48 h after CFA. Our findings provide evidence that inflammatory reactions are responsible for the recurrence of pain after NR1 KO in the SCDH.

Keywords

Inflammatory pain; N-methyl-D-aspartate receptor; Protein kinase Cγ; Mitogen activated protein kinases; p38; cyclooxygenase-2

Introduction

Chronic inflammatory pain is a major cause of disability in the world. There is strong evidence that peripheral inflammatory insults increase the excitability of spinal cord neurons, resulting in enhanced pain. This process involves the alteration of multiple neurotransmitters and

Please address all correspondence to: Hsinlin T Cheng, M.D., Ph.D, University of Michigan, Department of Neurology, 109 Zina Pitcher Place, Room 5015 BSRB, Ann Arbor, Michigan 48109-2200, 734-763-7276 (phone), 734-763-7275 (fax) email: chengt@umich.edu.
Section Editor : Dr. Linda Sorkin

intracellular signaling events in the spinal cord dorsal horn (SCDH) and is termed “central sensitization” (Woolf and Salter, 2000, Woolf, 2007).

Once SCDH sensory neurons are activated by an initial peripheral noxious stimulus, the depolarization of postsynaptic terminals in SCDH neurons triggers the activation of the N-methyl-D-aspartate (NMDA) receptor (Costigan and Woolf, 2000, Woolf and Salter, 2000). Membrane depolarization activates the NMDA receptor, removing magnesium blockade from the ion channel and allowing for the influx of calcium. The elevation of the intracellular calcium triggers a series of calcium-sensitive signal cascades, including protein kinase C (PKC) and mitogen activated protein kinases (MAPK) and ultimately leads to altered gene expression (Costigan and Woolf, 2000, Haddad, 2005). The end result of central sensitization is a prolonged postsynaptic depolarization in SCDH neurons that enhances nociceptive messages.

The NMDA receptor consists of tetramers of 2 NR1 subunits and 2 NR2 subunits. The NR1 subunit is required for this ionotropic glutamate receptor to function as an ion channel throughout the CNS including the SCDH. Previously, our laboratory developed a spatio-temporal knockout (KO) of the NR1 subunit that was confined to the lumbar (L4-L5) SCDH (South et al., 2003, Inturrisi, 2005). This spatial knockout was achieved using Cre-LoxP technology: The gene for Cre DNA recombinase was introduced by a recombinant adeno-associated viral vector (rAAV) microinjected into the spinal cord dorsal horn of NR1 floxed transgenic mice. This approach successfully deleted the NR1 gene and expression of the NMDA protein in the SCDH and served as a powerful tool to dissect regional NMDA receptor-dependent and -independent signaling events (South et al., 2003, Inturrisi, 2005).

NMDA receptor activation triggers multiple signaling pathways. One secondary messenger downstream of the NMDA receptor is PKCγ. PKCγ is an important mediator of pain behaviors in a variety of animal models (Malmberg et al., 1997, Basbaum, 1999). Mice with a deletion of the PKCγ gene exhibit less neuropathic pain than wild type controls (Malmberg et al., 1997). In inflammatory pain models, PKCγ also mediates phase 2 pain behaviors induced by formalin (Sweitzer et al., 2004). In SCDH, PKCγ is expressed by neurons within the inner layers of lamina II and lamina V that comprise a subset of NMDA-dependent spinal circuits underlying persistent pain (Basbaum, 1999, Polgar et al., 1999, Martin et al., 2001).

Mitogen activated protein kinases (MAPK) are a family of serine threonine kinases, the members of which include extracellular signal-regulated kinases (ERK1/2), p38, and c-jun N-terminal protein kinases (JNK). All members of the MAPK family are reported to mediate pain in the spinal cord (Ji et al., 2002, Svensson et al., 2003, Obata and Noguchi, 2004). Among these, ERKs 1 and 2 are activated by NMDA currents in the SCDH (Ji et al., 1999, Haddad, 2005). The activation of ERK1/2 induces phosphorylation of downstream transcription factors to alter gene expression. In contrast, p38 activation in the SCDH appears localized to microglia (Svensson et al., 2003). Microglial p38 activation mediates NMDA receptor-induced prostaglandin E2 release and hyperalgesia (Svensson et al., 2003). The activation of microglial p38 could upregulate cyclooxygenase (COX)-2 expression (N'Guessan et al., 2006). Since the p38-COX-2 pathway is not known to be a downstream signaling event of NMDA receptor activation, it could be a potential NMDA-independent mechanism mediating inflammatory pain.

In the current study, we observed that the protective effects of NR1 KO against inflammatory pain induced by Complete Freund’s adjuvant (CFA) diminished after 24 h. Since the NR1 subunit is permanently deleted in the SCDH of NR1 KO mice, there must be NMDA receptor-independent mechanisms that mediate the recurrence of pain. We have characterized the activation of PKCγ, ERK1/2, and p38, as well as COX-2 expression, in SCDH after CFA

injection and determined the signaling mechanisms that may contribute to the recurrence of pain in NR1 KO mice.

Experimental procedures

The floxed NMDA receptor I subunit (fNR1) gene was described previously (Tsien et al., 1996) . These mice have a loxP site placed in the intron between exons 10 and 11 and a second loxP site down stream after exon 22. The two loxP sequences flank a region of the NR1 gene which encodes the four membrane domains (three transmembrane (TM) domains and the M2 recurrent loop) and the entire C-terminal sequence of the polypeptide chain. Adult (30–40 gm) fNR1 mice of both sexes were used in these studies. The animals used for breeding the fNR1 line were tested for homozygosity of the loxP sites using Southern blot procedures, and the MAX-BAX (Charles River Laboratories, Wilmington, MA) background strain characterization procedure was used to identify breeders that were at of least 92–95% C57BL/6 background. Each study was approved by Institution Animal Care Committee of Weill Medical College, Cornell University.

The Cre-expressing rAAV vector

Construction, production, and purification of the Cre-expressing rAAV vector were as described by Kaspar and colleagues (Kaspar et al., 2002). The rAAV is a single stranded DNA parvovirus (4.7 kb) engineered without viral coding sequences. The inserted transgene included a cytomegalovirus promoter and the coding sequence for a fusion protein of green fluorescent protein (GFP)-Cre. Control animals received the same dosage of the rAAV-GFP vector that lacked the coding sequence for the Cre recombinase.

Intraparenchymal injection (IPI) of rAAV

Mice were anesthetized with ketamine-xylazine and placed in a spinal frame to support the abdomen and pelvis. Laminectomy was performed at the level of L2-3 and three unilateral injections of 1 μl (1X 10^6 viral particles/ml) were administered 0.5 mm apart, to the right side of the SCDH at the depth of 0.3 mm (SCDH), using a glass pipette with a 40 μm diameter tip attached to a 5 μl Hamilton syringe. The syringe was mounted on a microinjector (model 5000; David Kopf Instruments, Tujunga, CA) attached to a stereotaxic unit (model 960; David Kopf Instruments). Mice were evaluated as described below after at least 14 d post IPI administration of vehicle (PBS), rAAV-GFP-Cre, or rAAV-GFP.

Two weeks following the application of rAAV, inflammatory pain was induced by injecting 5 μl of Complete Freund's adjuvant (CFA, 1mg/ml of heat killed Mycobacterium tuberculosis in 85% paraffin oil and 15% mannide monoleate, Sigma) into the right hind paw of a lightly restrained mouse.

Mechanical stimulus threshold

The threshold for a non-noxious mechanical stimulus was assessed using a set of von Frey filaments. The animal was placed in a Plexiglas cage with mesh flooring and allowed to acclimate for 15 min. The filaments were applied perpendicularly against the midplantar surface of the foot. A predetermined mean von Frey hair was presented to each foot, and the subsequent presentation of additional filaments was determined using the up–down method of Dixon (Dixon, 1980). Although all responses were noted, counting of the critical 6 data points did not begin until the response threshold was first crossed. The resulting pattern of the 6 positive and negative responses was tabulated and 50% gram threshold was calculated using the formula provided by Chaplan and colleagues (Chaplan et al., 1994).

Cold (cooling stimulus) threshold

Cold sensitivity was assessed using the acetone drop application method (Bridges et al., 2001). Animals were placed in Plexiglas cages with mesh flooring at a level above the researcher and allowed to acclimate for 15 min. A drop of acetone was placed against the midplantar surface of each hind paw, and a positive response (score of 1) was recorded if the animal withdrew (flinched) the paw after application, whereas the absence of a response was given a value of 0. The score was the number of positive responses observed in five consecutive trials.

Immunohistochemistry

Following the intraplantar injection of 5 μl CFA or saline into the right hind paw, and behavioral testing (see below) the mice were perfused transcardially with 4% paraformaldehyde. The spinal cord was dissected and placed into 4% paraformaldehyde for 1 h prior to cryoprotection in 30 % sucrose for a minimum of 72 h. Spinal cords were rapidly frozen into a mold with mounting media (OCT). Twenty μm cryosections were cut using a cryostat. The sections were permeablized with 0.1 % Triton X100 in TBS and incubated with primary antisera overnight at RT. Subsequently, the sections were rinsed 3 X 10 min in TBS and incubated with secondary antiserum conjugated with different fluorophores (AlexaFluor 488, 594, or 647 Invitrogen, Carlsbad, CA) or biotin (Vector Laboratories, Burlingame, CA) for the avidin-biotin-peroxidase complex-3,3-diaminobenzidine tetrahydrochloride technique (Hsu et al., 1981, Cheng et al., 1996). The control slides were exposed to diluted normal goat serum instead of primary antibody. For quantification of ERK1/2 positive sensory neurons, seven sections from the L4 L6 lumbar spinal cord were randomly selected, and the numbers of pERK1/2-positive neurons in the superficial laminae (I II) were counted. Total 4 animals were counted for each condition with the person conducting the counting unaware of the treatment to avoid bias.

NR1 in situ hybridization

Slide-mounted spinal cord and DRG sections (12 μm) were hybridized with a 2.2 kb [^{33}P]UTP-labeled (Perkin-Elmer Life Sciences, Boston, MA) antisense or sense probe directed to the region of the NR1 subunit that includes the entire sequence that is flanked by the loxP sites. Hybridization was performed according to methods described previously (South et al., 2003). After the posthybridization washes, slides were dried by dehydration, dipped in NTB-2 emulsion from Eastman Kodak (Rochester, NY), and incubated at 4°C for 16–18 d. Slides were then developed and counterstained with hematoxylin and eosin.

Immunoblots

Following CFA or saline injection to right hind paws, lumbar spinal cords (L4-6) were dissected from mice anesthetized by isofluorane and rapidly homogenized with ice cold modified RIPA buffer (50 mM Tris-HCl, pH 7.4, 1% Nonidet P-40, 150 mM NaCl, 1 mM EDTA) with protease inhibitor cocktail (1:10, Sigma),1 mM sodium orthovanadate, and 1 mM sodium fluoride. The lysates were sonicated, centrifuged, and supernatants containing 50μg of protein from each sample were separated by SDS-PAGE and transferred to PVDF membranes. The membranes were rinsed, and incubated with primary antibodies overnight at 4°C. The next day, membranes were rinsed and incubated with HRP-conjugated secondary antibodies for 1 h at RT. The membranes were then rinsed and processed for ECL chemiluminescence and exposed to Hyperfilm (Amersham) for 30 sec to 10 min (Cheng et al., 2000a, Cheng et al., 2000b). Densitometry was performed using the Image J program and density for each protein was normalized to an actin loading control. Results were expressed as a fold change over the saline-treated control.

Antibodies

The primary rabbit polyclonal antibodies against phosphorylated(p) ERK1/2, ERK1/2, pp38, p38 and pPKCγ (1:1000 for immunoblots, and 1:100 for immunohistochemistry) were purchased from Cell Signaling Technology (Danvers, MA). Polyclonal rabbit antibody against PKCγ (1:1000 for immunoblots, and 1:500 for immunohistochemistry) was purchased from Santa Cruz Biotechnology (Santa Cruz, CA). Rabbit anti-COX-2 (1:1000 for immunoblots and 1:100 for immunohistochemistry), chicken anti-neuron specific enolase (NSE, 1:200) and rat monoclonal macrophage (1:500) antibodies were purchased from Abcam Inc. (Cambridge, MA). Rat monoclonal anti-OX42/CD11b antibody (1:500) and mouse anti-NeuN (1:500) was purchased from Invitrogen (Carlsbad, CA)

Data presentation and statistical analyses

All data are presented as group means + SEM. Where appropriate, between-group comparisons were made by unpaired student's t test or one-way ANOVA followed by a post hoc Tukey's multiple comparison test. A p of 0.05 value or less was considered statistically significant.

Results

Viral transduction and recombination in the SCDH

Two weeks after IPI of rAAV-GFP-Cre into the adult mouse lumbar spinal cord, a highly localized pattern of expression of GFP was observed, one that was restricted to the ipsilateral dorsal horn (circled area) and part of the ipsilateral ventral horn (Fig. 1A). Region-specific Cre-mediated recombination was evident where reduction in NR1 mRNA labeling was measured in an adjacent section (Fig. 1B) by *in situ* hybridization using an anti-sense riboprobe, the sequence of which spans the loxP sites that will be deleted by the Cre-mediated recombination (Tsien et al., 1996). The extent of the GFP label correlated almost perfectly with the area of reduced NR1 mRNA (Fig. 1A, B). Using this injection protocol, the entire ipsilateral dorsal horn was effectively depleted of NR1 mRNA, leaving the contralateral dorsal horn and nonlumbar spinal cord completely intact. This finding is consistent with our previously published data (South et al., 2003).

NR1 KO decreases mechanical and cold allodynia at 24 h, but not 48 h, after CFA injection

Two weeks after IPI, mechanical thresholds and cold sensitivity scores were measured and serve as the baseline comparisons before CFA injection (Fig. 2A, B). The spatial KO of NR1 was performed by IPI of rAAV-GFP-Cre (Cre) into the right side of the SCDH of adult NR1 floxed mice. For the control group, rAAV-GFP (GFP) was used for IPI. Hind paw injection with 5 μl of CFA reduced the mechanical thresholds in comparison to baseline 24 h after treatment (Fig. 2A). In parallel, CFA treatments induced cold allodynia presented as increased cold sensitivity score compared to baseline 24 h after treatment (Fig. 2B). CFA-induced mechanical and cold allodynia were detected in both Cre and GFP mice but the allodynia was significantly less in Cre than GFP mice, suggesting NR1 KO in the SCDH inhibited CFA-induced mechanical and cold allodynia at 24 h. However, the protective effects of NR1 KO were not significant 48 h after CFA injection (Fig. 2).

CFA induced PKCγ activation is inhibited by NR1 KO

To elucidate the signaling cascades underlying CFA-induced pain, we examined the potential for CFA-induced PKCγ activation to be dependent on NMDA receptor function. First, PKCγ immunohistochemistry was performed to localize PKCγ expression in the SCDH (Fig. 3A, B). In saline-injected control mice, PKCγ immunoreactivity was detected in neurons (arrows) and their processes (arrowheads) at the inner layer of lamina II (Fig. 3A, arrows). The PKCγ immunoreactivity in the ipsilateral SCDH within 10 min after CFA treatment demonstrated

similar anatomical distribution of PKCγ as saline treated mice (Fig. 3B, arrows). To quantify PKCγ activation, immunoblots of both PKCγ and pPKCγ were performed (Fig. 3C). CFA injection significantly increased the level of PKCγ protein expression in the ipsilateral SCDH in comparison to control (Fig. 3C). In addition, the level of expression of pPKCγ was also increased 10 min after CFA injection (Fig. 3C). To test the effects of NR1 KO on CFA-induced PKCγ activation, CFA was injected into both Cre and GFP mice. NR1 KO significantly reduced the levels of CFA-induced PKCγ phosphorylation 10 min after CFA treatment when compared with CFA-treated GFP mice (Fig. 3D, E). The inhibitory effects of NR1 KO on PKCγ last for at least 48 h (Fig. 3E).

CFA-induced ERK1/2 phosphorylation is inhibited by NR1 KO

We next examined the roles of ERK1/2, known downstream kinases of the NMDA receptor, in CFA-induced pain. The right halves of spinal cords were collected from NR1 floxed mice. To determine the time course of ERK1/2 phosphorylation following CFA, immunoblots of pERK1/2 were performed in no treatment and 10 min, 1 h, and 24 h after intraplantar CFA (Fig. 4A). Densitometric measurement demonstrated significant ERK phosphorylation 10 min after CFA with a maximum level (a 5.5 fold increase) activation detected at 1 h. The phosphorylation of ERK1/2 decreased by 24 h (Fig. 4B). The density of total ERK1/2 from each condition was used as the loading control. To study the roles of NR1 KO on peak CFA-induced pERK1/2 activation, pERK1/2 immunoblots were performed using spinal cords from GFP and Cre mice 1 h after CFA injection. Cre mice had significantly decreased levels of ERK1/2 phosphorylation following CFA treatment compared to the levels of saline treated control mice, whereas the same effects were not detected in GFP mice (Fig. 4C, D).

The anatomical distribution of pERK1/2 was examined by immunohistochemistry employing the same antibody used for the immunoblots. In GFP mice, pERK1/2 was detected in neurons of the superficial layer of the ipsilateral dorsal horn 10 min after intraplantar CFA (Fig. 5A). In contrast, pERK1/2 immunostaining was rarely detected in CFA treated Cre mice (Fig. 5B). Statistic evaluation indicated a 3.5 fold decrease of pERK1/2-positive neurons in Cre mice compared to GFP mice 10 min after CFA treatment (Fig. 5C). The inhibitory effects of NR1 KO on pERK1/2 phosphorylation in SCDH neurons lasted for at least 48 h (Fig. 5C).

Increased neuronal COX-2 expression in Cre mice after CFA treatment

We next investigated NMDA receptor-independent signaling events that could be responsible for the recurrence of pain 48 h after CFA treatment. COX-2 expression is a commonly detected marker of pain conditions in a variety of pain models. COX-2 expression and activation are not known to be NMDA-receptor dependent. COX-2 immunohistochemistry was performed to examine COX-2 expression in response to intraplantar CFA. COX-2 immunoreactivity was not detected in GFP mice with or without CFA treatment (data not shown). However, COX-2 expression was detected in macrophages of the spinal cord in saline treated Cre mice 48 h after CFA treatment (Fig. 6A, arrows). Moreover, CFA treatment induced intense COX-2 expression in neurons (Fig. 6B, arrowheads) of the ipsilateral SCDH, in addition to macrophages (arrows), 48 h after CFA injection (Fig. 6B). The neuronal staining was confirmed with double labeling by anti-neurons specific enolase (NSE) antibody (compare Fig. 6C and 6D). The neuronal COX-2 expression was not detected at 10 min and 24 h (data not shown). COX-2 immunoblots demonstrated increased COX-2 protein levels in saline treated Cre mice compared to GFP control (Fig. 6E, F). A maximal level (5 fold increase) of COX-2 was detected in CFA-treated Cre mice 48 h after CFA injection compared to GFP control (Fig. 6E, F).

Increased microglial p38 activation after NR1 KO

Spinal microglial p38 activation is demonstrated in a variety of painful conditions. Microglial activation is NMDA-independent and contributes to chronic pain. We next studied p38

activation 48 h after CFA treatment in GFP and Cre mice. Immunoblotting detected low pp38 levels in GFP mice (Fig. 7A). CFA treatment did not affect pp38 levels in GFP mice (Fig. 7A, B). However, pp38 levels were significantly elevated after intraplantar CFA, but not saline in Cre mice (Fig. 7A). To localize pp38 expression in SCDH, we performed pp38 immunohistochemistry 48 h after CFA treatment. Adjacent sections were processed for GFP, pp38, and OX42/CD11b (a microglial marker). GFP immunoreactivity was detected in SCDH neurons, confirming the neurons were infected with r-AAV-GFP-Cre (Fig. 7C). In serial adjacent sections, pp38 immunoreactivity was detected in cells (Fig. 7D) with features of microglia in SCDH and adjacent white matters (Fig. 7E). Double immunofluorescent studies with high power confocal microscopy was able to determine that OX42 antibody labeled the cellular processes of microglia (Fig. 7F, green) whereas pp38 was detected in the nuclei (Fig. 7F, red). Microglial p38 activation was not detected at 10 min and 24 h after CFA injection (data not shown).

Discussion

Spatio-temporal KO of the NR1 gene in the SCDH effectively eliminates NR1 expression and NMDA channel function (South et al., 2003). Although the effect of KO is permanent, the protection against CFA-induced allodynia is transient. This phenomenon is unique and has not been documented previously. Similar findings have not been observed in pain studies using intrathecal administration of NMDA receptor blockers, or antisense knockdown (Shimoyama et al., 2005). Our selective regional KO is specific for lumbar SCDH whereas the intrathecal administration of NMDA receptor inhibitors could affect the whole central nervous system. In addition, while our selective regional KO is specific for the lumbar SCDH, it also results in a permanent functional deletion of the NMDA receptor. This approach circumvents the transient pharmacokinetics often seen with intrathecal administration of NMDA receptor antagonists. NMDA receptor-independent mechanisms for post-incisional pain were proposed by Zahn and colleagues (Zahn et al., 2005). Their reports suggest non-NMDA ionotropic excitatory amino acid receptors, instead of NMDA receptor, mediate dorsal horn neuronal sensitization after incision. Using the spatial NR1 KO, we are able to dissect regional spinal molecular events and characterize spinal pain mechanisms that are independent of NMDA receptor.

The current findings strongly suggest early PKCγ activation is dependent on NMDA receptor function. A similar finding was reported in the hippocampus. PKCγ activation and relocation to the cell membrane and dendritic branches of hippocampal neurons are dependent upon diacylglycerol and NMDA receptor-mediated calcium influx (Codazzi et al., 2006). Our findings are consistent with other published data, suggesting that PKCγ is NMDA receptor-dependent in the SCDH and does not participate in the recurrence of allodynia 48 h after CFA treatment in our NR1 KO model.

NMDA receptor activation induces ERK1/2 phosphorylation in a variety of systems (Haddad, 2005). ERK1/2 activation contributes to inflammatory pain by induction of NK1 and prodynorphine expression (Ji et al., 2002). In the current study, pERK1/2 is located to the lamina I of the SCDH, consistent with published data by Ji and colleagues (Ji et al., 2002). Here we report ERK1/2 activity is attenuated by NR1 KO in SCDH, suggesting ERK1/2 is regulated in a NMDA receptor-dependent manner within 48 hr after CFA treatment and does not participate in the recurrence of pain 48 h after CFA treatment. Our findings are supported by Ji and colleagues, who demonstrated that the NMDA receptor blocker MK801 attenuates the ERK1/2 activation in the superficial SCDH after capsaicin treatment (Ji et al., 1999). In addition to NMDA receptor mediated ERK1/2 activation, metabotropic glurtamate receptor (mGlu) 1 and 5 could also activate ERK1/2 in spinal cord dorsal horn neurons by subcutaneous injection of formalin (Karim et al., 2001). Interestingly, the mGlu-mediated nocifensive behaviors require persistent ERK activation 7 days after 10 μl CFA treatment (Adwanikar et

al., 2004). However, we did not detect significant ERK1/2 activation in our NR1 KO mice, suggesting there is no significant mGlu-mediated ERK activation following low dose CFA treatment.

We found enhanced COX-2 expression in Cre mice before CFA treatment in macrophages. It is possible that injection of rAAV could induce a certain degree of inflammation. However, this is very unlikely due to lack of COX-2 upregulation in GFP mice. COX-2 expression in invading macrophages was reported in the peripheral nerves following traumatic injuries (Ma and Eisenach, 2003). Although the mechanism of macrophage activation in Cre mice is still unknown, our findings suggest NMDA independent mechanisms are involved. CFA injection triggers additional release of glutamate in the SCDH, which normally would bind to NMDA receptors. In the absence of NMDA receptors, the CFA induced increased levels of glutamate in SCDH would likely bind to other glutamate receptors and/or glutamate transporters. Glutamate could induce neuronal COX-2 expression, as reported by Strauss and colleagues in cultured cerebellar granular cells (Strauss et al., 2000). In their report, glutamate-induced COX-2 expression is mediated by both NMDA and kainate receptors. Therefore, we may have observed kainate receptor-mediated COX-2 upregulation in SCDH neurons following CFA treatment.

Spinal microglial activation is detected in multiple pain models. However, most of this evidence is derived from models of neuropathic pain (Inoue, 2006). Nerve injury-induced microglial activation is likely mediated by ATP through purinergic receptors (Inoue, 2006). A high dose (0.1 ml) of CFA injection to hind paws also induces microglial activation in rats (Raghavendra et al., 2004). This microglial activation is associated with increased astrocytes and elevation of proinflammatory cytokines (Raghavendra et al., 2004). We did not detect significant microglial activation in GFP mice with 5 μl of CFA injection, indicating CFA induced microglial activation is probably dose-dependent. The mechanism of microglial activation after NR1 KO is unclear. Our results suggest that it is a NMDA independent event. Microglia express glutamate transporters, and are activated by glutamate via the metabotropic glutamate receptors in cell culture (Taylor et al., 2005). Activated microglia release tumor necrosis factor-α (TNF-α) and Fas ligand which could stimulate adjacent sensory neurons to increase pain (Taylor et al., 2005).

Peripheral nerve injury induces spinal cord microglial p38 activation (Tsuda et al., 2004). Microglial p38 activation is dependant on nerve activity and could be a downstream event of P_2X_7 or P_2X_4 ATP receptors (Tsuda et al., 2004, Inoue, 2006, Wen et al., 2007). It is unknown how NR1 KO promotes microglial p38 activation after CFA treatment. One of the potential mechanisms could be that NR1 KO increases local interleukin-1β production which, in turn, triggers p38 activation in microglia (Sung et al., 2005). In addition, microglial p38 activation could lead to upregulation of inducible nitric oxide synthase and promote pain (Sung et al., 2005).

In summary, our unique approach of spatio-temporal NR1 KO provides a powerful tool to assess local events in the SCDH that mediate CFA-induced pain. We observe activation of NMDA receptor-dependent pathways, including PKCγ and ERK1/2, and the activation of inflammatory mechanisms, including COX-2 expression and microglial p38 activation. Our findings provide evidence that NMDA receptor blockade is not enough to complete relieve chronic inflammatory pain. The most effective treatment for chronic inflammatory pain can only be achieved by approaches that target multiple mechanisms, covering both NMDA-dependent and -independent pathways.

Acknowledgements

The authors would like to thank Paigee Chou and Ann Gregus for technical assistance and Barbara Inturrisi for secretarial support. Supported in part by NIDA grants: DA001457 and DA000198 (CEI), NIDA training grant: DA007274 (DEH), and NCI (T32) Training Grant: CA-009461-21 (HTC).

Abbreviations

NMDA
N-methyl-D-aspartate

NR1
NMDA receptor I subunit

KO
knockout

SCDH
spinal cord dorsal horn

CFA
Complete Freund's adjuvant

PKC
protein kinase C

ERK
extracellular signal-regulated kinase

COX
cyclooxygenase

rAAV
recombinant adeno-associated viral vector

MAPK
mitogen activated protein kinase

JNK
c-jun N-terminal protein kinase

TM
transmembrane

green fluorescent protein
GFP

IPI
intraparenchymal injection

NSE
neuron specific enolase

pERK
phosphorylated ERK

pPKC
phosphorylated PKC

phosphorylated p38
pp38

References

Adwanikar H, Karim F, Gereau RWt. Inflammation persistently enhances nocifensive behaviors mediated by spinal group I mGluRs through sustained ERK activation. Pain 2004;111:125–135. [PubMed: 15327816]

Basbaum AI. Spinal mechanisms of acute and persistent pain. Regional anesthesia and pain medicine 1999;24:59–67. [PubMed: 9952097]

Bridges D, Ahmad K, Rice AS. The synthetic cannabinoid WIN55,212–2 attenuates hyperalgesia and allodynia in a rat model of neuropathic pain. Br J Pharmacol 2001;133:586–594. [PubMed: 11399676]

Chaplan SR, Bach FW, Pogrel JW, Chung JM, Yaksh TL. Quantitative assessment of tactile allodynia in the rat paw. J Neurosci Methods 1994;53:55–63. [PubMed: 7990513]

Cheng HL, Steinway M, Delaney CL, Franke TF, Feldman EL. IGF-I promotes Schwann cell motility and survival via activation of Akt. Mol Cell Endocrinol 2000a;170:211–215. [PubMed: 11162904]

Cheng HL, Steinway ML, Russell JW, Feldman EL. GTPases and phosphatidylinositol 3-kinase are critical for insulin-like growth factor-I-mediated Schwann cell motility. The Journal of biological chemistry 2000b;275:27197–27204. [PubMed: 10829021]

Cheng HL, Sullivan KA, Feldman EL. Immunohistochemical localization of insulin-like growth factor binding protein-5 in the developing rat nervous system. Brain Res Dev Brain Res 1996;92:211–218.

Codazzi F, Di Cesare A, Chiulli N, Albanese A, Meyer T, Zacchetti D, Grohovaz F. Synergistic control of protein kinase Cgamma activity by ionotropic and metabotropic glutamate receptor inputs in hippocampal neurons. J Neurosci 2006;26:3404–3411. [PubMed: 16571747]

Costigan M, Woolf CJ. Pain: molecular mechanisms. J Pain 2000;1:35–44. [PubMed: 14622841]

Dixon WJ. Efficient analysis of experimental observations. Annu Rev Pharmacol Toxicol 1980;20:441–462. [PubMed: 7387124]

Haddad JJ. N-methyl-D-aspartate. NMDA) and the regulation of mitogen-activated protein kinase (MAPK) signaling pathways: a revolving neurochemical axis for therapeutic intervention? Prog Neurobiol 2005;77:252–282. [PubMed: 16343729]

Hsu SM, Raine L, Fanger H. Use of avidin-biotin-peroxidase complex (ABC) in immunoperoxidase techniques: a comparison between ABC and unlabeled antibody (PAP) procedures. J Histochem Cytochem 1981;29:577–580. [PubMed: 6166661]

Inoue K. The function of microglia through purinergic receptors: neuropathic pain and cytokine release. Pharmacology & therapeutics 2006;109:210–226. [PubMed: 16169595]

Inturrisi CE. The role of N-methyl-D-aspartate (NMDA) receptors in pain and morphine tolerance. Minerva anestesiologica 2005;71:401–403. [PubMed: 16012411]

Ji RR, Baba H, Brenner GJ, Woolf CJ. Nociceptive-specific activation of ERK in spinal neurons contributes to pain hypersensitivity. Nat Neurosci 1999;2:1114–1119. [PubMed: 10570489]

Ji RR, Befort K, Brenner GJ, Woolf CJ. ERK MAP kinase activation in superficial spinal cord neurons induces prodynorphin and NK-1 upregulation and contributes to persistent inflammatory pain hypersensitivity. J Neurosci 2002;22:478–485. [PubMed: 11784793]

Karim F, Wang CC, Gereau RWt. Metabotropic glutamate receptor subtypes 1 and 5 are activators of extracellular signal-regulated kinase signaling required for inflammatory pain in mice. J Neurosci 2001;21:3771–3779. [PubMed: 11356865]

Kaspar BK, Vissel B, Bengoechea T, Crone S, Randolph-Moore L, Muller R, Brandon EP, Schaffer D, Verma IM, Lee KF, Heinemann SF, Gage FH. Adeno-associated virus effectively mediates conditional gene modification in the brain. Proc Natl Acad Sci U S A 2002;99:2320–2325. [PubMed: 11842206]

Ma W, Eisenach JC. Cyclooxygenase 2 in infiltrating inflammatory cells in injured nerve is universally up-regulated following various types of peripheral nerve injury. Neuroscience 2003;121:691–704. [PubMed: 14568029]

Malmberg AB, Chen C, Tonegawa S, Basbaum AI. Preserved acute pain and reduced neuropathic pain in mice lacking PKCgamma. Science 1997;278:279–283. [PubMed: 9323205]

Martin WJ, Malmberg AB, Basbaum AI. PKCgamma contributes to a subset of the NMDA-dependent spinal circuits that underlie injury-induced persistent pain. J Neurosci 2001;21:5321–5327. [PubMed: 11438608]

N'Guessan PD, Hippenstiel S, Etouem MO, Zahlten J, Beermann W, Lindner D, Opitz B, Witzenrath M, Rosseau S, Suttorp N, Schmeck B. Streptococcus pneumoniae induced p38 MAPK- and NF-kappaB-dependent COX-2 expression in human lung epithelium. Am J Physiol Lung Cell Mol Physiol 2006;290:L1131–1138. [PubMed: 16414978]

Obata K, Noguchi K. MAPK activation in nociceptive neurons and pain hypersensitivity. Life Sci 2004;74:2643–2653. [PubMed: 15041446]

Polgar E, Fowler JH, McGill MM, Todd AJ. The types of neuron which contain protein kinase C gamma in rat spinal cord. Brain Res 1999;833:71–80. [PubMed: 10375678]

Raghavendra V, Tanga FY, DeLeo JA. Complete Freunds adjuvant-induced peripheral inflammation evokes glial activation and proinflammatory cytokine expression in the CNS. Eur J Neurosci 2004;20:467–473. [PubMed: 15233755]

Shimoyama N, Shimoyama M, Davis AM, Monaghan DT, Inturrisi CE. An antisense oligonucleotide to the N-methyl-D-aspartate (NMDA) subunit NMDAR1 attenuates NMDA-induced nociception, hyperalgesia, and morphine tolerance. J Pharmacol Exp Ther 2005;312:834–840. [PubMed: 15388787]

South SM, Kohno T, Kaspar BK, Hegarty D, Vissel B, Drake CT, Ohata M, Jenab S, Sailer AW, Malkmus S, Masuyama T, Horner P, Bogulavsky J, Gage FH, Yaksh TL, Woolf CJ, Heinemann SF, Inturrisi CE. A conditional deletion of the NR1 subunit of the NMDA receptor in adult spinal cord dorsal horn reduces NMDA currents and injury-induced pain. J Neurosci 2003;23:5031–5040. [PubMed: 12832526]

Strauss KI, Barbe MF, Marshall RM, Raghupathi R, Mehta S, Narayan RK. Prolonged cyclooxygenase-2 induction in neurons and glia following traumatic brain injury in the rat. J Neurotrauma 2000;17:695–711. [PubMed: 10972245]

Sung CS, Wen ZH, Chang WK, Chan KH, Ho ST, Tsai SK, Chang YC, Wong CS. Inhibition of p38 mitogen-activated protein kinase attenuates interleukin-1beta-induced thermal hyperalgesia and inducible nitric oxide synthase expression in the spinal cord. J Neurochem 2005;94:742–752. [PubMed: 16033422]

Svensson CI, Hua XY, Protter AA, Powell HC, Yaksh TL. Spinal p38 MAP kinase is necessary for NMDA-induced spinal PGE(2) release and thermal hyperalgesia. Neuroreport 2003;14:1153–1157. [PubMed: 12821799]

Sweitzer SM, Wong SM, Peters MC, Mochly-Rosen D, Yeomans DC, Kendig JJ. Protein kinase C epsilon and gamma: involvement in formalin-induced nociception in neonatal rats. J Pharmacol Exp Ther 2004;309:616–625. [PubMed: 14762097]

Taylor DL, Jones F, Kubota ES, Pocock JM. Stimulation of microglial metabotropic glutamate receptor mGlu2 triggers tumor necrosis factor alpha-induced neurotoxicity in concert with microglial-derived Fas ligand. J Neurosci 2005;25:2952–2964. [PubMed: 15772355]

Tsien JZ, Huerta PT, Tonegawa S. The essential role of hippocampal CA1 NMDA receptor-dependent synaptic plasticity in spatial memory. Cell 1996;87:1327–1338. [PubMed: 8980238]

Tsuda M, Mizokoshi A, Shigemoto-Mogami Y, Koizumi S, Inoue K. Activation of p38 mitogen-activated protein kinase in spinal hyperactive microglia contributes to pain hypersensitivity following peripheral nerve injury. Glia 2004;45:89–95. [PubMed: 14648549]

Wen YR, Suter MR, Kawasaki Y, Huang J, Pertin M, Kohno T, Berde CB, Decosterd I, Ji RR. Nerve Conduction Blockade in the Sciatic Nerve Prevents but Does Not Reverse the Activation of p38 Mitogen-activated Protein Kinase in Spinal Microglia in the Rat Spared Nerve Injury Model. Anesthesiology 2007;107:312–321. [PubMed: 17667577]

Woolf CJ. Central sensitization: uncovering the relation between pain and plasticity. Anesthesiology 2007;106:864–867. [PubMed: 17413924]

Woolf CJ, Salter MW. Neuronal plasticity: increasing the gain in pain. Science 2000;288:1765–1769. [PubMed: 10846153]

Zahn PK, Pogatzki-Zahn EM, Brennan TJ. Spinal administration of MK-801 and NBQX demonstrates NMDA-independent dorsal horn sensitization in incisional pain. Pain 2005;114:499–510. [PubMed: 15777875]

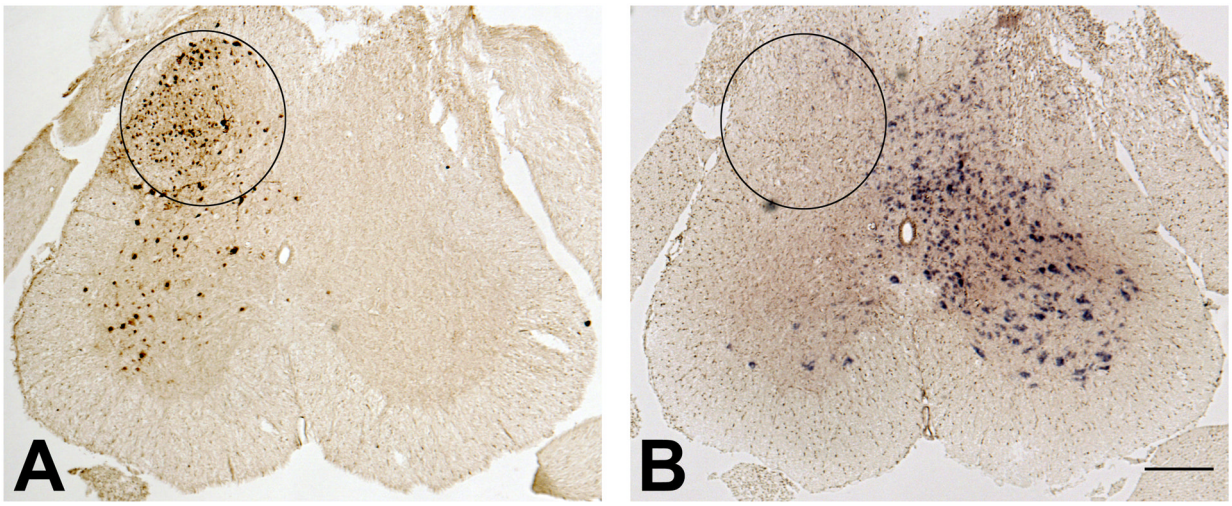

Figure 1.

IPI of rAAV-GFP-Cre into the SCDH of a floxed NR1 mouse results in viral transduction, Cre-mediated recombination, and a spatiotemporal knock-out of the NR1 gene. (A) On the side ipsilateral to the injection of rAAV-GFP-Cre, viral transduction results in the expression of GFP immunoreactivity in the SCDH (circled area). (B) Decreased NR1 gene expression as measured by *in situ* hybridization in the circled area of SCDH in an adjacent section, demonstrating successful NR1 KO. Bar = 250 μm.

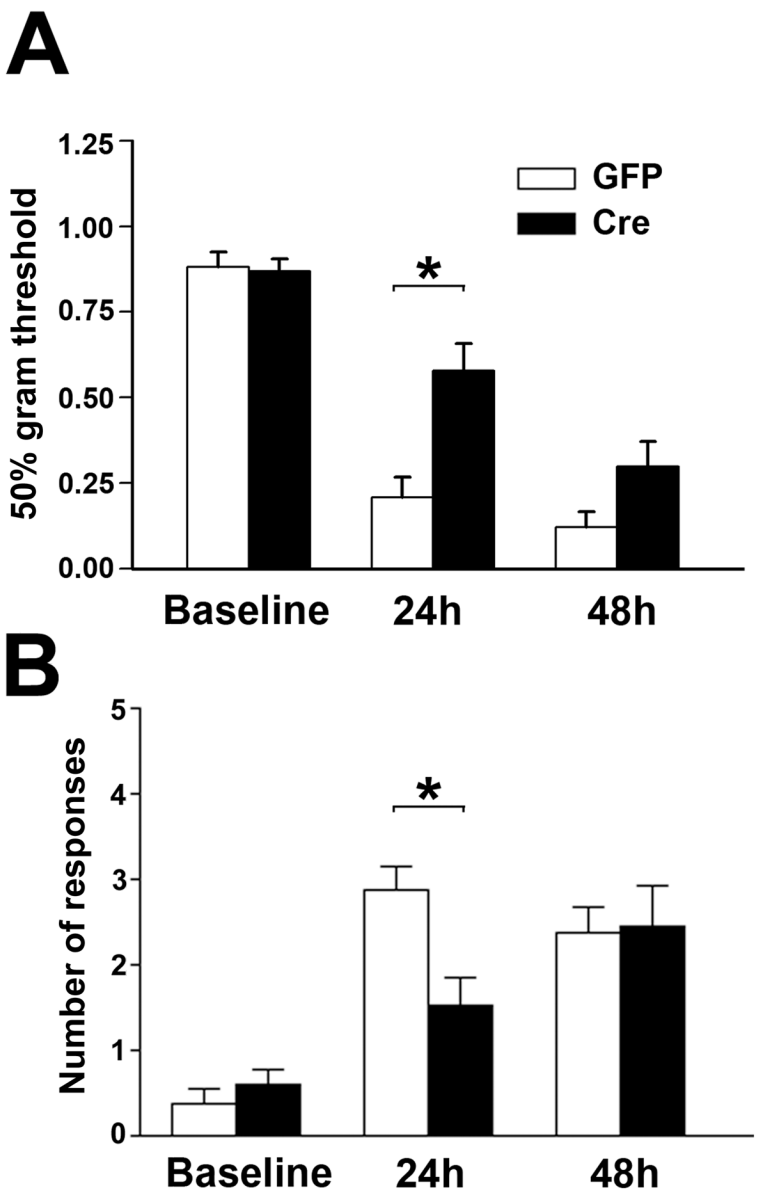

Figure 2.

Mechanical allodynia (A) and cold allodynia (B) resulting from the intraplantar injection of CFA are significantly attenuated at 24 h but not 48 h after CFA treatment in mice with a spatial KO of NR1 in the SCDH (Cre). (A) Mechanical allodynia was measured as a reduction in the baseline mechanical threshold (50% gm threshold) using von Frey hairs applied to the CFA treated paw while (B) Cold allodynia was measured as an increase in the number of responses after applying a drop of acetone to the CFA treated paw. Measurements were made before (baseline) and 24 and 48 hours after intraplantar CFA. Baseline values were not altered in GFP (n = 8) or Cre (n = 13) mice when measured before and after ipsilateral viral vector injection into the SCDH (data not shown). Data are the mean ± SEM (*p< 0.05).

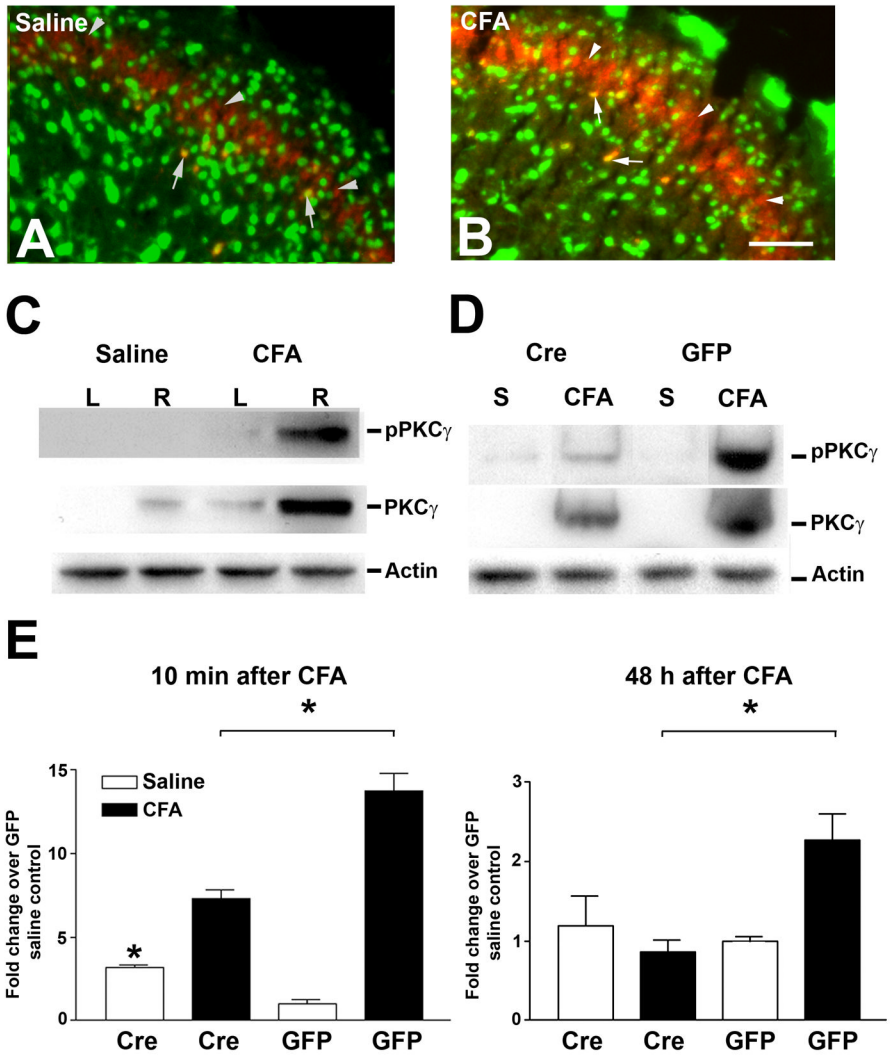

Figure 3.

CFA-induced activation of PKCγ and its phosphorylation in the SCDH are attenuated in NR1 KO (Cre) mice at 1h and 48 h after CFA treatments. Confocal images of lumbar SCDH sections show the expression of PKCγ (red) and NeuN (green) 10 min after intraplantar saline (A) or CFA (B) Bar = 50 μm. PKCγ expression was detected in the inner layer of lamina II (arrowheads) while neuronal PKCγ expression is show as yellow labeling (arrows). (C) Immunoblots of lumbar SCDH samples at 10 min after the injection of intraplantar saline or CFA into the right (R) paw of NR1 floxed mice show increased expression of pPKCγ and PKCγ ipsilateral to the CFA injected paw. (D) Immunoblots of samples of the right lumbar SCDH collected at 10 min after the injection of intraplantar saline (S) or CFA into the right paw of GFP or Cre mice show decreased expression of pPKCγ and PKCγ in the SCDH of Cre mice. Actin immunoblots serve as loading controls. (E) Densitometric analysis of pPKCγ immunoblots. The data were normalized to saline treated GFP mice. The CFA induced expression of pPKCγ in lumbar SCDH is significantly reduced at 10 min and 48 h after intraplantar CFA in Cre compared to GFP mice. Data are the mean ± SEM (n = 3) (* $p < 0.05$).

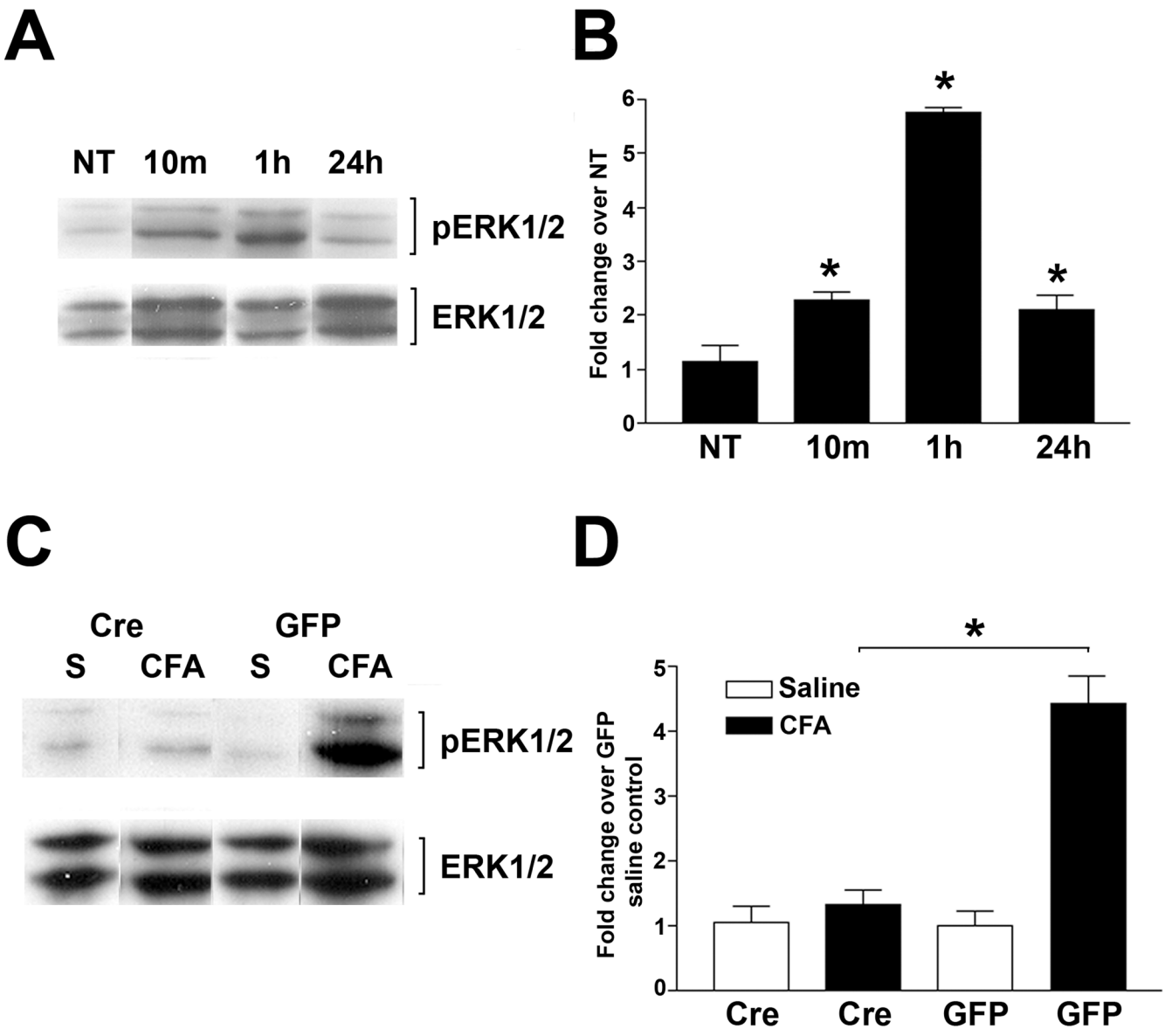

Figure 4.

CFA-induced activation of phospho (p) ERK1/2 in the SCDH is attenuated in NR1 KO (Cre) mice. (A) The time course of ERK1/2 and pERK1/2 after intraplantar CFA. Immunoblots of pERK1/2 in samples of the right lumbar SCDH of NR1 floxed mice before and at 10 min, 1 h, and 24 h after no treatment (NT) or intraplantar CFA. (B) Densitometric analysis of the immunoblots for pERK1/2 after treatments as described in (A). Data are normalized to the band intensity of total ERK1/2 and presented as the fold change over the untreated control (NT). (C) Immunoblots of pERK1/2 and ERK1/2 in samples of the right lumbar SCDH at 1 h after the injection of intraplantar saline (S) or CFA into the right paw of GFP or Cre mice. (D) Densitometric analysis of the immunoblots for pERK1/2 at 1 h after treatment as described in (C) shows the attenuation of CFA-induced pERK1/2 activation in Cre compared to GFP mice. Data are normalized to the band intensity of total ERK1/2 and presented as the fold change over the saline treated control. Data are the mean ± SEM (n = 3) (* $p < 0.05$).

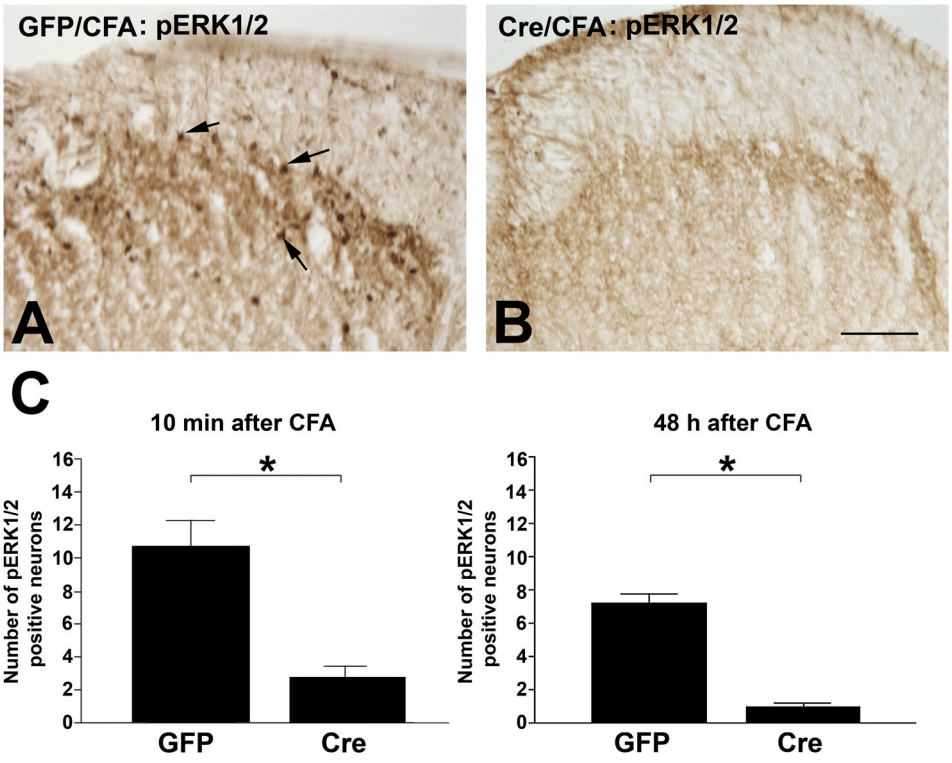

Figure 5.

CFA-induced activation of phospho (p) ERK1/2 is attenuated in pERK1/2 labeled neurons in the SCDH of NR1 KO (Cre) mice 10 min and 48 h after CFA treatments. Immunolabeling of pERK1/2 in the right lumbar SCDH of GFP (A) and Cre (B) mice at 10 min after intraplantar CFA. pERK1/2 labeled neurons (arrows) were detected in the superficial layers of the SCDH in Control (A) but not Cre (B) mice, Bar = 50 μm. Representative images from n = 4 animals per group. (C) The number of CFA–induced pERK1/2 labeled neurons is significantly reduced in Cre compared to GFP mice after 10 min and 48 h after CFA treatments. Data are the mean ± SEM (* $p < 0.05$).

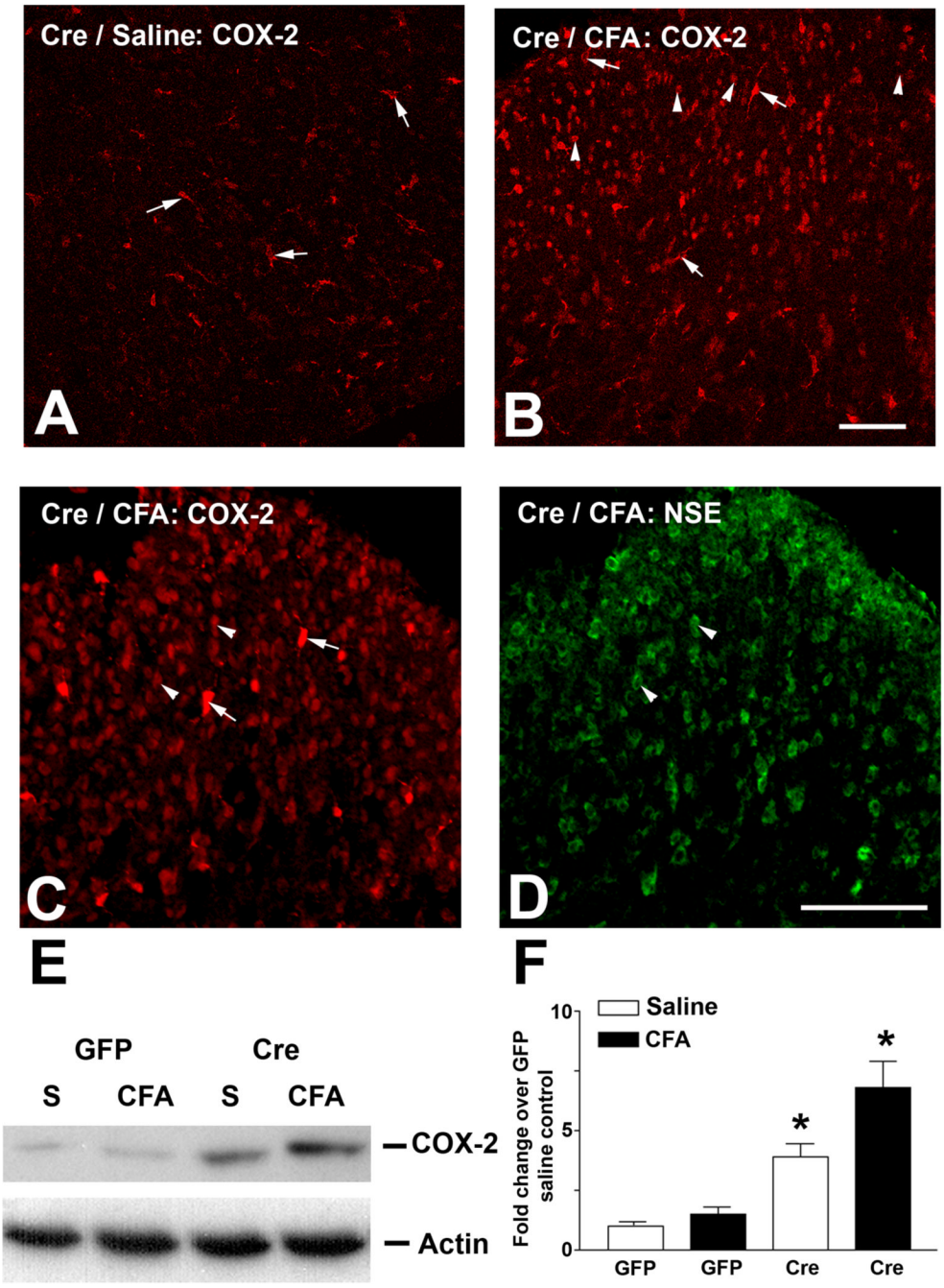

Figure 6.

COX-2 expression is upregulated in the SCDH of NR1 KO (Cre) mice. Sections of the right lumbar SCDH were obtained from Cre mice at 48 h after the intraplantar injection of saline (A, Cre/saline) or CFA (B, Cre/CFA) and labeled for COX-2. Saline treated Cre mice show COX-2 expression in macrophages (arrows) (A), while CFA treated Cre mice show COX-2 expression in both macrophages (arrows) and neurons (arrowheads) (B), Bar = 50 μm. The neuronal expression of COX-2 in CFA-treated Cre mice (C, arrowheads) was confirmed by double labeling with anti-NSE (D, arrowheads). E: Immunoblots demonstrate an enhanced expression of COX-2 in Cre compared to GFP mice 48 h after CFA treatment as described above. F: Densitometric analysis of COX-2 immunoblots demonstrates increased COX-2

expression in Cre mice 48 h after CFA treatment. The highest level of COX-2 expression was seen in Cre mice after CFA injection. Data are the mean ± SEM (n = 3) (* $p < 0.05$).

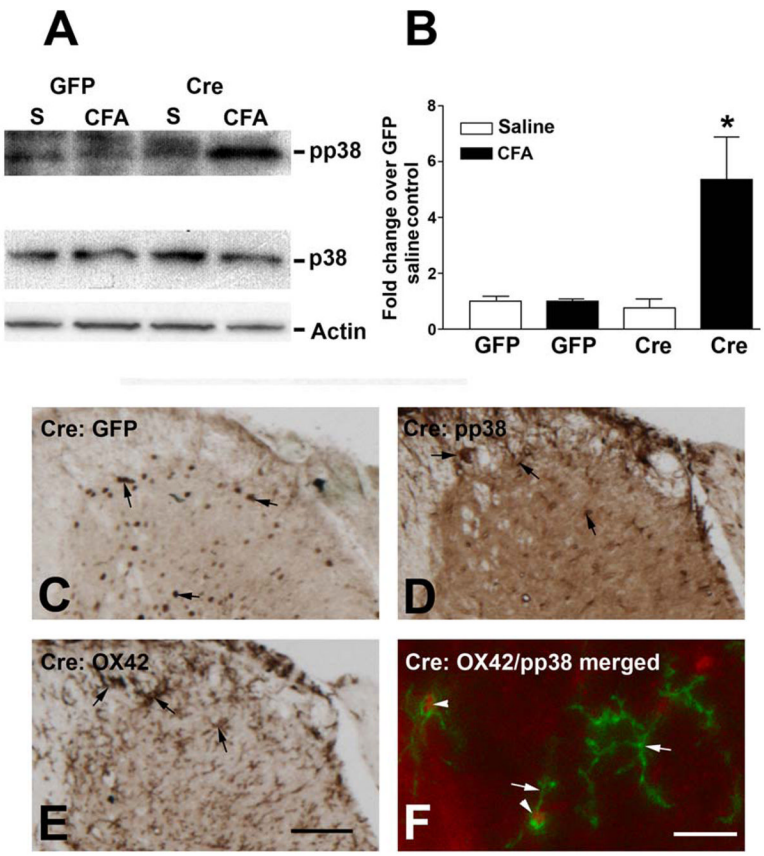

Figure 7.

Phospho(p)p38 is activated by CFA in the SCDH of NR1 KO (Cre) mice. (A) Immunoblots of pp38 and p38 in samples of the right lumbar SCDH at 48 h after the injection of intraplantar saline (S) or CFA into the right paws of GFP or Cre mice. (B) Densitometric analysis of the immunoblots shows that increased expression of pp38 was only seen in CFA-treated Cre mice. (C) The expression of GFP in the SCDH of a Cre mouse. (D) pp38 labeling of an adjacent section shows pp38 expression in the nuclei of microglia (arrows). (E) OX42 labels the cell membrane and processes of microglia on an adjacent section (arrows). (E) Confocal microscopy shows labeling of pp38 (red) and OX42 (green) and demonstrates that pp38 was activated in microglial nuclei (arrowheads). In contrast, OX42 labeled the cell processes (arrows). C, D, E, bar = 50 μm F, bar = 15 μm. Representative images from n = 4 animals per group.